

Mitigation of autogenous shrinkage in alkali activated slag mortars by internal curing

A. R. Sakulich · D. P. Bentz

Received: 28 June 2012 / Accepted: 19 November 2012 / Published online: 29 November 2012
© RILEM 2012

Abstract Alkali activated slag shows considerable promise as an environmentally friendly alternative to binders produced from ordinary portland cement. The shrinkage behavior of alkali activated slags, however, is not well understood, and is a hurdle to widespread adoption. The use of pre-wetted lightweight aggregate-based internal curing to mitigate shrinkage in slags activated by Na_2CO_3 solution or waterglass/NaOH solution has been investigated. Chemical shrinkage measurements were used to determine the amount of additional curing water needed by the mixtures, and autogenous and total shrinkage measurements used to determine the effects of internal curing on the overall shrinkage of the systems. Internal curing can completely mitigate autogenous shrinkage; however, in the systems examined here, drying shrinkage was the dominant shrinkage factor. In such a case, the benefits of internal curing are most clearly observed during the first 7 days.

Keywords Slag · Shrinkage · Alkali activation · Internal curing

1 Introduction

Production of 1 ton of ordinary portland cement (OPC) releases roughly between 0.5 and 1 ton of CO_2 into the atmosphere and consumes 4–5 GJ of energy [28, 50]. Due to the large quantities of OPC (~3.3 billion tons) produced annually, cement production is the third largest producer of greenhouse gas (accounting for roughly 5–8 % of global anthropogenic totals) and consumes about 5 % of the global primary industrial energy supply [21, 36, 47].

A great deal of research has therefore gone into developing more environmentally friendly alternative binders, each with their own unique properties. Calcium aluminate cements (CACs) display excellent chemical resistance and acceptable strength, but are less economically viable, have a controversial history (several building collapses were initially, and incorrectly, blamed on CAC, and the material was subsequently banned in many building codes), and decrease in strength at later ages under several curing scenarios, as metastable reaction products are converted into stable phases [32]. Calcium sulfoaluminate (CSA) cement, when compared to OPC-based binders, is easier to grind, is fired at temperatures roughly 200 °C lower than OPC, and releases less greenhouse gas during the firing process. However, CSA is at an economic disadvantage due to the use of bauxite as a principal raw material (as in CACs), and undergoes more substantial volumetric changes (i.e. shrinkage or

A. R. Sakulich (✉) · D. P. Bentz
Engineering Laboratory, National Institute of Standards
and Technology, Stop 7313, Gaithersburg,
MD 20899-7313, USA
e-mail: a.sakulich@gmail.com

D. P. Bentz
e-mail: dale.bentz@nist.gov



expansion) during curing [32, 48]. CSA cements are, however, widely employed in nations such as China.

Supersulfated cements, produced from alkaline blast furnace slags with high Al_2O_3 contents, calcium sulfate, and an alkaline activator were widely used in the mid-twentieth century, but usage has decreased as changes in ore refining began producing slags not chemically appropriate as raw materials [19, 25]. In addition to a lowered environmental impact, supersulfated cements have relatively low heat of hydration and perform well in aggressive environments, but sometimes require prolonged curing due to low initial strength and possible carbonation issues [49]. A European standard for supersulfated cements is now available [42].

Alkali-activated binders formed primarily of low-calcium aluminosilicate reactants are generally referred to as ‘geopolymers’ (and occasionally soil cements, alkaline inorganic polymers, hydroceramics, zeocements/zeoceramics, or alkali activated natural pozzolans) [23, 33]. Most frequently produced from waste materials such as fly ash, these binders are reported to have excellent durability, a substantially reduced environmental impact, and are beginning to enter the market in both major and niche applications [20, 22, 39]. As with other systems, ‘geopolymers’ suffer from a lack of long-term performance and durability data, as well as a possible susceptibility to carbonation issues, a difficulty in handling highly alkaline activators in practical applications, and an incompatibility with admixtures commonly used in OPC-based systems [27, 38].

Another alternative binder that shows promise is alkali activated slag, which has a long history in northern Europe, Scandinavia, and the Soviet Union [51]. Alkali activation of slag produces primarily calcium silicate hydrates (C–S–H) similar to those found in OPC, distinct from the zeolite-like ion-balanced structure of geopolymers [44]. Although alkali activated slags have been reported to have excellent strength [40], durability [51], and chemical resistance [9, 10], the production of practical alkali activated slag binders on commercial scales remains elusive.

One factor limiting alkali activated slag binders is shrinkage, which is both more substantial in alkali activated slag than in OPC and less well understood [35]. Shrinkage can take two forms: drying shrinkage, where water leaves the system through evaporative

processes, or autogenous shrinkage, which does not involve water exiting the system. Autogenous shrinkage is closely related to chemical shrinkage, which occurs when the initial reactants in the hydration processes have a greater volume than the final products. This leads to the creation of empty pores as hydration reactions continue after setting; initially saturated with solution, some of the pores self-desiccate, leading to the formation of menisci that cause tensile stresses (analogous to drying shrinkage). These stresses then ‘pull’ the pore walls inwards, leading to a measurable shrinkage, i.e. autogenous shrinkage. While some studies have identified drying shrinkage as being the dominant mechanism at work in alkali activated slags [44], others have pointed to autogenous shrinkage as being dominant [34]. A recent study by Thomas et al. [45] determined that slags activated by a sodium silicate solution were likely to undergo twice as much chemical shrinkage as comparable OPC-based systems.

Internal curing is a method that counteracts autogenous shrinkage by providing additional water, to reduce self-desiccation and relieve tensile stresses inside pores within the hydrating cement paste [12]. The amount of additional water that is potentially needed can be calculated through the measurement of chemical shrinkage [11, 13]. In internal curing, a water reservoir is used, commonly either a superabsorbent polymer [30, 31] or an absorbent lightweight aggregate (LWA) such as pumice or expanded clay [1, 46]. As the internal humidity of the system drops, water is released from the reservoir and self-desiccation of the hydrating cement paste is prevented, while concurrently promoting continuing hydration of the cement particles. Because the LWA are dispersed uniformly (theoretically), the system can be evenly cured, as opposed to the use of ‘external curing’ (wet burlap, etc.) that only provides additional water to the exposed surfaces of the system.

This study investigates internal curing via LWA as a shrinkage mitigation technique in three mortars: a control OPC mortar, a slag activated by Na_2CO_3 solution, and a slag activated by a waterglass/NaOH solution. Chemical shrinkage was measured to determine the amount of internal curing needed in each case. Autogenous and total shrinkages, along with compressive strength and heat evolution (via isothermal calorimetry), were measured for mixtures with and without internal curing. In one mortar (the slag



activated by Na_2CO_3 solution) internal curing with only water and internal curing using the activating solution were compared.

2 Materials and methods¹

Three different mixtures without internal curing were investigated: a OPC-based control mixture (mixture C); slag activated by a Na_2CO_3 solution (mixture S); and slag activated by a waterglass/sodium hydroxide solution (mixture W). The following reactants were used in these mixtures: ASTM C150 Type I cement; granulated ground blast furnace slag (GGBFS); waterglass; anhydrous NaOH; distilled water; a blend of four normal weight sands previously used in studies involving LWA [14] designated ‘S16’, ‘ASTM C778 20/30’, ‘ASTM C778 graded’, and ‘F95’ as fine aggregate; and a commercially available expanded clay LWA satisfying the requirements of standard ASTM C330 [5]. The chemical compositions of the cement, slag, and waterglass can be found in Table 1; particle size distributions of selected reactants can be found in Fig. 1; and the proportioning of mixtures C, S, and W can be found in Table 2. The LWA was prepared by combining it with water on a shaker-mixer for 1 h, followed by soaking for 23 h. As the size fractions of both the LWA and normal weight aggregates were known, LWA was incorporated by removing an appropriate volume of each of the four normal weight sands used as aggregate to avoid significantly altering the overall aggregate size distribution. The activator:binder mass ratio was fixed at 0.45 for mixtures C and S, and at 0.55 for mixture W in order to obtain similar workabilities; fine aggregate made up 55 % of total volume of all mortar mixtures. (The term activator:binder is used here in place of water:cement, since the alkali-activated slags are not cement, and the liquid used to activate them is not water.)

Preparation of the mortars was carried out as described in ASTM C109 [8]. After 24 h the cubes

Table 1 Reactant chemical compositions, % by mass, as reported by the manufacturers

	Cement	GGBFS	Waterglass
CaO	62.1	42.1	–
SiO ₂	20	34.6	26.4
MgO	4.6	6.6	–
Al ₂ O ₃	4.1	11.7	–
SO ₃	2.8	1.3	–
Fe ₂ O ₃	2.7	0.51	–
H ₂ O	2.3	–	65.4
Na ₂ O	–	–	8.2

GGBFS granulated ground blast furnace slag

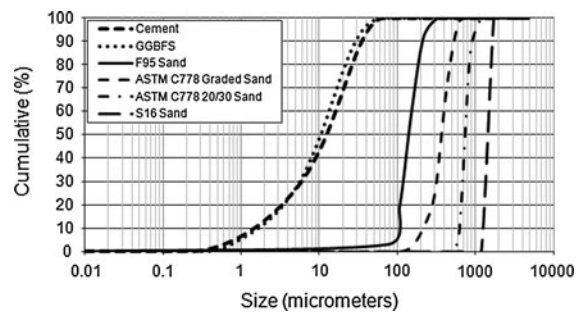


Fig. 1 Particle size distribution of Type I cement, granulated ground blast furnace slag (GGBFS) and four normal weight sands used as aggregate. The curve of the F95 sand is aberrant below 10 % cumulative due to the relatively small number of data points available for this curve

were demolded and submerged in lime-saturated water until testing. Compression tests were carried out on at least three specimens at ages of 3, 7, and 28 days.

Isothermal calorimetry tests were carried out over the course of 7 days at 25 °C. Initially, samples were taken from batches used to prepare compression testing specimens, placed in a glass vial, sealed, and loaded in the calorimeter. This ‘standard mode’ used a 45 min wait time after sample loading to allow the temperature inside the calorimeter to equilibrate. The initial results (not shown) showed the presence of a ‘tail’ on the left side of each calorimetric curve due to this equilibration period of the calorimeter. Because the device waits before collecting data, so as to negate the effects of the cell being exposed to the outside environment, heat production due to early-age chemical reactions was not observed. The experiments were therefore re-run with an in situ mixing apparatus, in which slag or cement powder was placed, dry, into a

¹ Certain commercial equipment, instruments, or materials are identified in this report in order to specify the experimental procedure adequately. Such identification is not intended to imply recommendation or endorsement by the National Institute of Standards and Technology, nor is it intended to imply that the materials or equipment identified are necessarily the best available for the purpose.

Table 2 Mortar mixture proportions

	Activator mixture name	Control (C)	Waterglass/NaOH (W)	Na ₂ CO ₃ (S)
Binder	Type I cement (g)	2,000	–	–
	GGBFS (g)	–	2,000	2,000
Aggregate	F95 (g)	1,318	1,318	1,318
	ASTM C778 20/30 (g)	1001.78	1001.78	1001.78
	ASTM C778 graded (g)	1001.78	1001.78	1001.78
	S16 (g)	1,950	1,950	1,950
Activator	Water (g)	900	–	–
	Waterglass/NaOH solution (g)	–	1,100	–
	Na ₂ CO ₃ solution (g)	–	–	900

GGBFS granulated ground blast furnace slag

glass vial. A device consisting of two pipettes containing either activating solution or water and a disposable plastic stirrer connected to a drive shaft was then inserted into the top of the glass vial. (Initial (unpublished) tests by the authors using only a glass vial and alkaline activator show that the glass and the high-pH solution either do not react, or react so little as to be below the detection limit of the calorimeter.)

The slag or cement powder and the activating solution were brought to thermal equilibrium in the calorimeter prior to mixing. After 45 min was allowed to elapse so that the calorimeter temperature could equilibrate, the activating solution was then squeezed from the pipettes and the stirrer engaged. In this way, heat generated due to initial reactions (particle wetting, initial dissolution, etc.) was also quantified.

Chemical shrinkage was evaluated using ASTM standard C1608 [4]. Approximately 10 g of fresh paste was placed in a glass vial to create a roughly 10–15 mm thick layer; the vial was then filled with distilled water and topped with a rubber plug through which a graduated capillary tube had been inserted. A drop of paraffin oil was added to the top of the tube to prevent evaporation and the whole apparatus was placed in a temperature-controlled bath maintained at 25 °C. Chemical shrinkage can be used to estimate the amount of internal curing water that will be needed to address autogenous shrinkage using an equation first published by Bentz et al. [11, 13]:

$$M_{LWA} = \frac{C_f \cdot CS \cdot \alpha_{max}}{S \cdot \phi_{LWA}} \quad (1)$$

where M_{LWA} is the mass of LWA needed per unit volume of concrete (kg/m³); C_f is the cement factor of

the concrete or mortar (kg/m³); CS is the ultimate chemical shrinkage of the cement or binder (g H₂O/g cement or binder powder); α_{max} is the expected maximum degree of hydration of the cement; S is the degree of saturation of the aggregate; and ϕ_{LWA} is the absorption of the LWA (kg H₂O/kg dry LWA).

The expected maximum degree of hydration was not measured here. Previous research [41] showed 21 ± 1.5 and 27.4 ± 0.9 % of slag was left unreacted in similar waterglass/NaOH- and Na₂CO₃ activated mixtures, respectively. The expected degree of hydration for these two mixtures is then estimated to be 79 and 72.5 %, respectively. A typical value for a control mixture with a water:cement ratio of 0.45 at late ages (>90 days) would be close to 100 % [24]. The specific gravity of cement (3.15 g/cm³) and slag (2.71 g/cm³) powders were measured in accordance with ASTM Standard C188 [3] (using isopropanol in place of kerosene) and a cement factor of $C_f = 562.6$ kg/m³ was thus computed.

C_f , CS , and α_{max} , essentially dictate the amount of water that is required for successful internal curing. The denominator of Eq. 1 represents the LWA that is required to carry that water into the mixture. The water absorption of the aggregate at 24 h, ϕ_{LWA} , and the amount of water that will be readily released by the aggregate during desorption to 93 % RH, were measured to be 26.5 kg H₂O/kg dry LWA and 0.95 %, respectively, in a previous study [13]. For internal curing, a higher value of desorption is always better; low values indicate that the aggregate will not release water even at a reduced relative humidity, preventing the water from interacting with the cement. For many LWAs of the expanded clay type produced



in the U.S., their desorption behaviors are quite similar [17].

It should be noted that the chemical shrinkage measurements may suffer slightly from the length of time that elapses between the mixing of the paste and the first reading (roughly 5–10 min.). Shrinkage that occurs during this time is not measured; however, as this length of time is substantially (h) less than the final set time of the mixes, this is not likely to have a significant effect.

After the chemical shrinkage results were collected, Eq. 1 was used to determine the composition of four additional mixtures: C(IC), S(IC)a, S(IC)b, and W(IC). These mixtures are the control mixture with internal curing, the Na_2CO_3 activated mixture with water as the internal curing agent, the Na_2CO_3 activated mixture with Na_2CO_3 solution as the internal curing agent, and the waterglass/NaOH activated mixture with internal curing, respectively. The compositions of these four mixtures can be found in Table 3. The amount of LWA used in each mixture is 5 % more than the minimum required as a safety factor.

Autogenous shrinkage was measured in accordance with ASTM standard C1698, using corrugated plastic tubes [6]. At least three replicate test specimens of each mixture were cast, stored in an environmental chamber at 25 ± 3 °C, and measured hourly for the first 8 h, and at least three times a week thereafter. Determination of the initial length is critical in autogenous shrinkage measurements. Using the first

value, obtained at 1 h after mixing, led to highly variable data, as the material in the corrugated tubes had not yet set and the measurement was affected by how the tube was placed in the length comparator. Instead, the initial length was chosen to be the first length measurement obtained after the mixture's initial set time, determined (by qualitative observation supported by calorimetric measurement) to be 4 h for mixture C, 24 h for mixture S, and 1 h for mixture W. Although shrinkage occurs before set has been established, this shrinkage can generally be accommodated by deformation of the still-fluid cement paste. Shrinkage after set is the shrinkage that can lead to cracking and a reduction of mechanical properties, therefore, choosing to begin measurements at the mixture's set time provides data that may not include pre-set shrinkage, but includes shrinkage likely to be of interest in practical applications.

Total drying shrinkage was measured using the procedure outlined in ASTM standard C596 [7]. Prisms were cast in steel molds roughly 25 mm × 25 mm × 285 mm, wrapped in plastic, and placed in an environmental chamber. The prisms were demolded after 1 day and, due to logistical constraints, allowed to cure submerged in limewater for 7 days instead of the 3 days as recommended in ASTM C596. (Mixtures activated by Na_2CO_3 were an exception; after 1 day of curing, the samples were still relatively soft and often broke during demolding. As such, they were demolded after 2 days of curing, instead of 1 days.) During drying in a 23 °C, 50 % RH

Table 3 Proportioning of mortars containing lightweight aggregate for internal curing

	Activator mixture name	Control C(IC)	Waterglass/NaOH W(IC)	Na_2CO_3 S(IC)a	Na_2CO_3 S(IC)b
Binder	Type I cement (g)	2,000	–	–	–
	GGBFS (g)	–	2,000	2,000	2,000
Aggregate	F95 (g)	1,190	1189.4	1158.2	1158.2
	ASTM C778 20/30 (g)	835.6	833	823.6	823.6
	ASTM C778 graded (g)	881	879.6	714.6	714.6
	S16 (g)	1491.6	1482.2	1,065	1,065
	LWA (g)	370	626	268	268
Activator	Water (g)	900	–	–	–
	Water, LWA (g)	100	170	72	–
	Solution, LWA (g)	–	–	–	72
	Waterglass/NaOH solution (g)	–	1,100	–	–
	Na_2CO_3 solution (g)	–	–	900	900

GGBFS granulated ground blast furnace slag



environment, prisms were measured with at least 24 h between measurements over the course of 28 days of drying.

3 Results

3.1 Strength

The compressive strength (Fig. 2) of the control mixture (C) increased from 9.1 ± 1.9 MPa at 3 days to 60.4 ± 3.2 MPa at 28 days; the Na_2CO_3 activated mixture (S) increased from 33.9 ± 1.6 MPa at 3 days to 60.7 ± 3.7 MPa at 28 days; and the waterglass/NaOH activated mixture (W) had a significantly higher compressive strength at all ages, increasing from 67.4 ± 3.5 MPa at 3 days to 114.2 ± 6.3 MPa at 28 days.

Internal curing reduced the compressive strengths of all mixtures, most prominently at early ages (Fig. 2). The decrease in strength observed with the incorporation of internal curing is due primarily to mechanical considerations: the LWA is simply not as strong an aggregate as normal weight sand. Other effects, such as differences in paste/aggregate bonding when LWA is used in place of sand or the effect of age on paste/aggregate bonding cannot be discounted, and may also have an effect, but were not investigated here.

Mixture C(IC) reached strengths of 31 ± 1.3 and 53.3 ± 5.1 MPa after 3 and 28 days of curing, decreases of 30 and 12 %, respectively when compared to the control mixture. The two Na_2CO_3

activated mixtures, S(IC)a and S(IC)b, which contained water and Na_2CO_3 solution as the internal curing agents, achieved roughly similar strengths of 28 ± 1.6 and 25.6 ± 0.5 MPa after 3 days, and 53.8 ± 2.8 and 56.6 ± 3.1 MPa after 28 days, respectively. Therefore, the nature of the internal curing agent, whether water or activating solution, had no significant effect on compressive strength. Mixture W(IC) had higher compressive strengths than any of the other internally cured mixtures (60.6 ± 7.3 and 88.6 ± 5.4 MPa after 3 and 28 days of curing, respectively), although these strengths were 10 and 22 % lower than the compressive strength of mixture W without internal curing. Compressive strengths of mixtures with and without internal curing can be influenced by both mixture proportions and the specific curing conditions employed [26]; limewater immersion was used here.

The substantially higher strengths of waterglass/NaOH activated mixtures are possibly due to the much higher pH of the activating solution, which more completely dissolves slag and thus produces more strength bearing phases. The waterglass also provides the system with a relatively large amount of highly reactive SiO_2 that encourages the rapid formation of strength-bearing phases, primarily C–S–H [40, 41].

3.2 Calorimetry

The use of the in situ mixing apparatus enabled quantification of the heat flow (Fig. 3) and cumulative heat evolution (Fig. 4) from the moment activating solution came in contact with slag or cement powder.

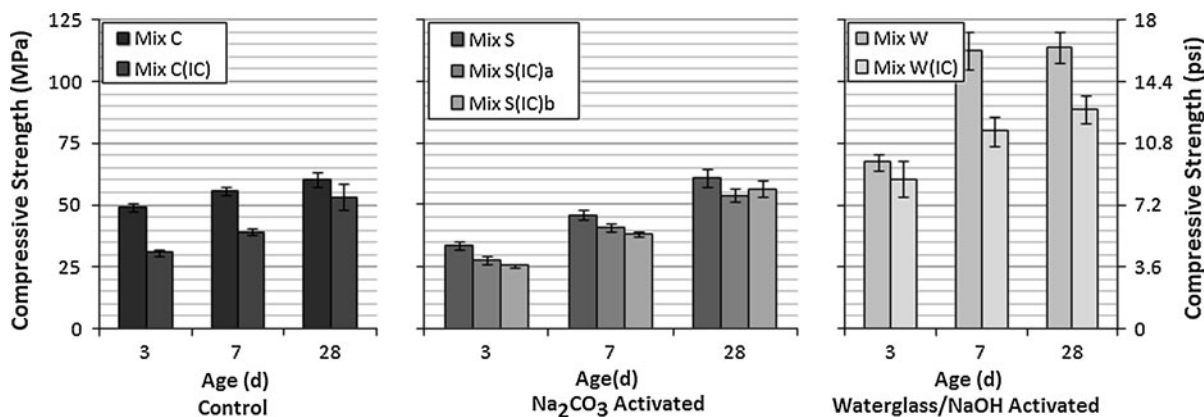


Fig. 2 Compressive strengths of the control, Na_2CO_3 activated, and waterglass/NaOH activated mixtures (C, S, and W, respectively) at ages of 3, 7, and 28 days with and without internal curing. All scales are equal. Error bars represent standard deviation

Initial peaks observed during the early period (i.e., the first hour; Figs. 3, 4, inset) represent the initial dissolution of ionic species from the slag or cement, followed by gelation into calcium silicates and other phases (primarily aluminates). This occurs quite rapidly in mixture C, which reaches a heat evolution value of nearly 18 mW/g of binder within the first quarter-hour; mixtures S and W reach a maximum heat flow of roughly 5 mW/g of binder, but the peaks of these two mixtures are much broader and somewhat bimodal, suggesting several reactions are occurring. At an age of 1 h, the cumulative heat evolution of mixtures C and W are roughly equal, at about 12 mW/g of binder. This value, in turn, is twice that of mixture S after 1 h.

Secondary peaks observed at later ages represent the bulk hydration of calcium silicates and the formation of binding phases such as C–S–H or, in the case of the alkali-activated slags, impure C–S–H containing Ca and Si substituted by Na and Al, respectively [15]. Mixture C exhibits a broad secondary peak lasting from roughly 6 to 11 h; mixture S exhibits a similar peak, albeit of lower magnitude, from 9 to 17 h. Such a peak cannot be observed in mixture W, and heat flow related to the initial peak decreases much less rapidly, suggesting the initial and secondary peaks may overlap. If so, bulk hydration and the formation of binding phases would occur at very early ages, supported by the qualitative

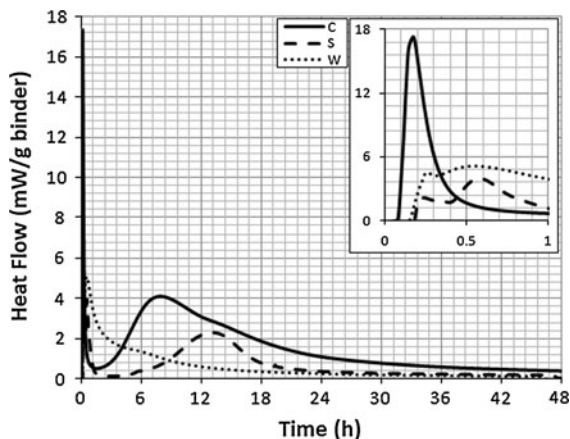


Fig. 3 Heat flow of the control, Na_2CO_3 activated, and waterglass/NaOH activated mixtures (C, S, and W, respectively) over the initial 48 h as determined by isothermal calorimetry with an in situ mixing attachment. *Inset* Heat flow over only the first hour. Units of the *inset axes* are the same as the larger figure, and are omitted for clarity

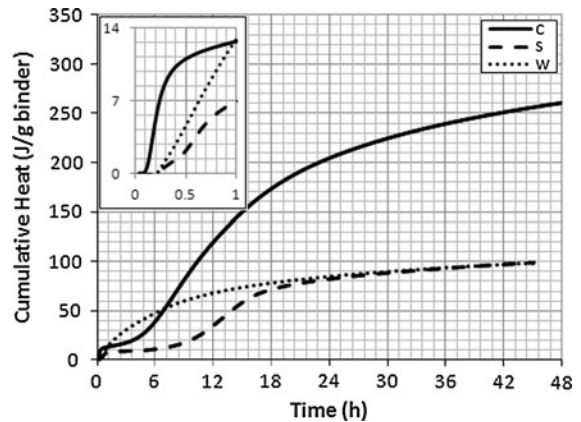


Fig. 4 Cumulative heat evolution of the control, Na_2CO_3 activated, and waterglass/NaOH activated mixtures (C, S, and W, respectively) over the initial 48 h as determined by isothermal calorimetry with an in situ mixing attachment. *Inset* Cumulative heat evolution over only the first hour. Units of the *inset axes* are the same as the larger figure, and are omitted for clarity

observation that mixture W sets and gains strength much more rapidly than the other two mixtures. While the cumulative heat evolution of mixtures S and W eventually level off around 100 J/g binder at 48 h, the cumulative heat evolution of mixture C reaches a value more than $2.5\times$ greater.

It should be mentioned that the calorimetric curves of mixtures containing internal curing (not shown here) are almost identical in shape and size to those of mixtures without internal curing, except that they have, generally speaking, slightly greater values (a matter of no more than roughly two or three percent). This slight increase is due to the fact that internal curing water can be used to create additional hydration products and produce a higher degree of hydration.

Relating isothermal calorimetry curves to strength gain is extremely difficult. In the two slag-based mixtures, S and W, cumulative heat evolution is almost identical at ages greater than 20 h, but mixture W has a substantially higher compressive strength. It is known that strength development in alkali-activated slags is limited by the nucleation and growth of ionic species [29]; however, nucleation and growth have very little effect on heat evolution. A recent review by Bullard et al. [16] notes that, in OPC-based systems, the dissolutions of C_3S and C_3A into various ionic species are strongly exothermic ($\Delta H = -137.6$ and -248.3 kJ/mol, respectively), whereas the

precipitation of C–S–H(I) and C–S–H(II) from ionic solutions is relatively weak ($\Delta H = \sim -20$ kJ/mol). This means that a substantially larger amount of C–S–H can be precipitated in one system compared to another, with little noticeable difference in heat evolution. Of the two possible origins of the increased compressive strength of mixture W over mixture S, the production of strength-bearing C–S–H-like phases due to the presence of soluble silica is therefore likely to have a greater effect than increased dissolution of ions due to higher pH (which would also have a strong effect on heat evolution).

A number of factors complicate the discussion of alkali activated slags and calorimetry in regards to the extant literature. The variable nature of the chemical composition and amorphous content of slags, as well as the different activators/curing processes used by different researchers, limits comparisons to noting that other researchers [2, 43] have observed calorimetric curves of generally similar size and shape for their particular alkali-activated slags.

3.3 Chemical shrinkage

Mixtures C and S reached similar levels of chemical shrinkage (~ 0.0465 mL H₂O/g binder) after 6 days (Fig. 5). The bulk of the chemical shrinkage in mixture C occurred during the first 24 h, with a more gradual rate in mixture S, which did not level off until 48 h. This is in keeping with the much slower bulk hydration of mixture S, as observed by isothermal calorimetry. The rate of shrinkage in mixture W was virtually identical to that of mixture C for the first 6 h, after which the rate of shrinkage began to level off. The shrinkage of mixture W was between those of mixtures C and S until an age of 40 h; after this point, mixture W exhibited the lowest cumulative chemical shrinkage.

The values of the different variables (including those determined by chemical shrinkage measurements) used in Eq. 1 are shown in Table 4 and were used to proportion the mixtures containing internal curing.

The high pH of the activator for mixture W leads to a more ‘complete’ reaction than in the other mixtures, that is, it leads to the production of more hydration products. Because chemical shrinkage occurs when final reaction products occupy less volume than initial reactants, more reaction products can lead directly to

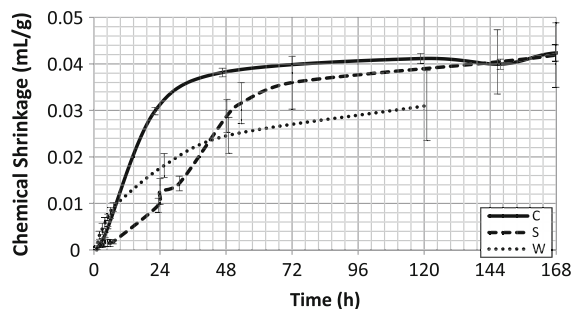


Fig. 5 Chemical shrinkages of the control, Na₂CO₃ activated, and waterglass/NaOH activated mixtures (C, S, and W, respectively) over the first week. Error bars represent standard deviation

higher chemical shrinkage. However, the activating solution of mixture W also contains a large amount of reactive silica, which creates an expansive silica gel that would not be seen in the other mixtures. This gel does not necessarily contribute to compressive strength, but may expand to fill a portion of the pore space, thus reducing observed chemical shrinkage. All three mixtures, therefore, have similar chemical shrinkage because they have a similar amount of unfilled pore space, even though the extent of reaction between mixtures C and S and mixture W are significantly different.

Slag hydration also leads to the refinement of the pore structure; many small pores are created, and these pores have been identified as one of the factors leading to the enhanced durability properties of alkali activated slag binders [35]. However, smaller pores create larger stresses if they are partially emptied during self-desiccation, which can lead to greater autogenous shrinkage. Another factor involves the pore solution; the activating solution used with mixture W was much more viscous than either the water used to activate mixture C or the Na₂CO₃ solution used to activate mixture S. Higher viscosity pore solution may lead to higher surface tension of the meniscus of a partially-filled pore, and thus higher autogenous shrinkage.

The chemical shrinkage of mixtures containing internal curing were also measured (not shown). Theoretically, internal curing should have no effect on the chemical shrinkage of samples that are completely ‘externally cured’ in water baths; as pores are created due to chemical shrinkage, the pores will fill with external water, which can be absorbed automatically, rather than water trapped in the LWA,

Table 4 Variables used to determine the mass of LWA required for internal curing (M_{LWA})

Mixture variable	Unit	Control (C)	Waterglass/NaOH (W)	Na ₂ CO ₃ (S)
C_f	kg/m ³	589.4	562.63	518.43
CS	kg H ₂ O/kg cement	0.0465	0.0465	0.1
α_{MAX}	n/a	0.7	0.72	0.79
S	n/a	0.265	0.265	0.265
ϕ_{LWA}	kg H ₂ O/kg LWA	0.95	0.95	0.95
M_{LWA}	kg/m ³	108.87	72.71	162.68

which will not be released until internal humidity decreases slightly. In practice, however, ‘complete’ external curing is impossible, and internal curing has a substantial effect, lowering the extent of chemical shrinkage observed here by over 50 %. Some locations in the sample volume (say, at the bottom of the vial) are relatively ‘far’ from external curing water. Internal humidity in these areas will drop long before external curing water can arrive at the site, these pores will absorb water from the LWA, less external water will be absorbed, and there will be a much smaller difference noted in the capillary tube (i.e. the chemical shrinkage measurement will be lower), along with the emptying of pores within the LWA that are providing water locally.

3.4 Autogenous shrinkage

After the first few days, the autogenous shrinkage of mixture C was constant at roughly 0.03 % (Fig. 6). In the two alkali activated mixtures, S and W, autogenous shrinkage continuously increased in magnitude to roughly 0.15 and 0.25 %, respectively, over the course of 28 days. Although all three had similar levels of chemical shrinkage, indicating a similar amount of unfilled pore space, autogenous shrinkage is affected by the pore size distribution (smaller pores in the alkali-activated slags lead to higher stresses and thus higher autogenous shrinkage) and the composition of the pore solution (increasing pore solution viscosity, which is lowest in mixture C and highest in mixture W, also leads to higher stresses and thus higher autogenous shrinkage. Pore solution molarity may also have an effect on which pores empty first, though this is not clear).

Mixtures C(IC), S(IC)a, and S(IC)b, were fairly consistent, with autogenous strains measured close to zero, indicating the efficacy of the internal curing

proportioned into these mixtures. Mixture W(IC) seems to have undergone a slight autogenous expansion, as evidenced by an average autogenous *expansion* of approximately 0.025 %. The reason for this is unclear, but is likely related to the abundance of reactive silica in the activating solution; with extra water provided by internal curing, enough expansive, Si-rich gel could be produced that would lead to overall expansion. Another possibility is that the LWA, an aluminosilicate clay, is reacting with the high pH of the activating solution to create geopolymer-like products. (This scenario is unlikely, as a preliminary experiment in which LWA was exposed to activating solution inside a calorimeter cell resulted in the release of no appreciable amount of heat.) Future microstructural and chemical analyses are needed to answer this question more definitively.

At least one trend is clear: internal curing effectively eliminates autogenous shrinkage in alkali activated slags. The mechanism by which this is achieved is the same in alkali activated slags as it is in OPCs: the additional liquid desorbed by the LWA during curing enters the binder paste pores, preventing self-desiccation and eliminating the larger magnitude tensile forces that lead to autogenous shrinkage.

3.5 Total shrinkage

The measurements of chemical shrinkage and autogenous shrinkage occur in sealed containers with limited interaction with the outside environment; total shrinkage specimens, however, are rectangular prisms that undergo all forms of shrinkage, including drying shrinkage.

The control mixture (Fig. 7) had the lowest total shrinkage, increasing to about 0.05 % after 7 days and roughly 0.075 % after 28 days. Internal curing made little difference at early ages; at 21 days, however, the

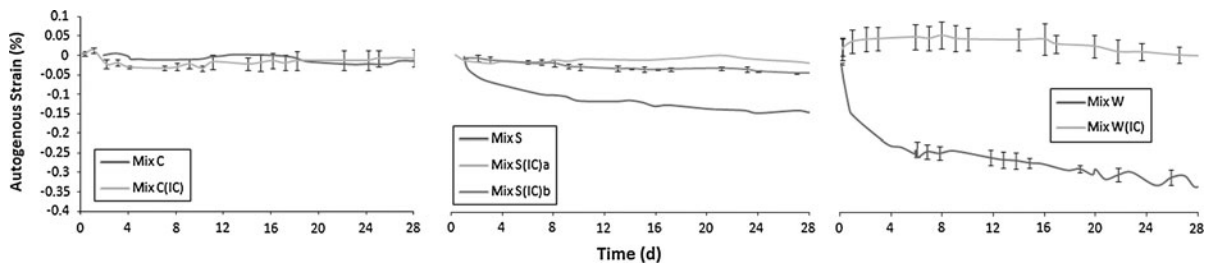


Fig. 6 Autogenous strains of the control, Na_2CO_3 activated, and waterglass/NaOH activated mixes (mixes C, S, and W, respectively) with and without internal curing. All scales are

equal. *Error bars* represent measured standard deviation; *curves without error bars* are an average of two specimens

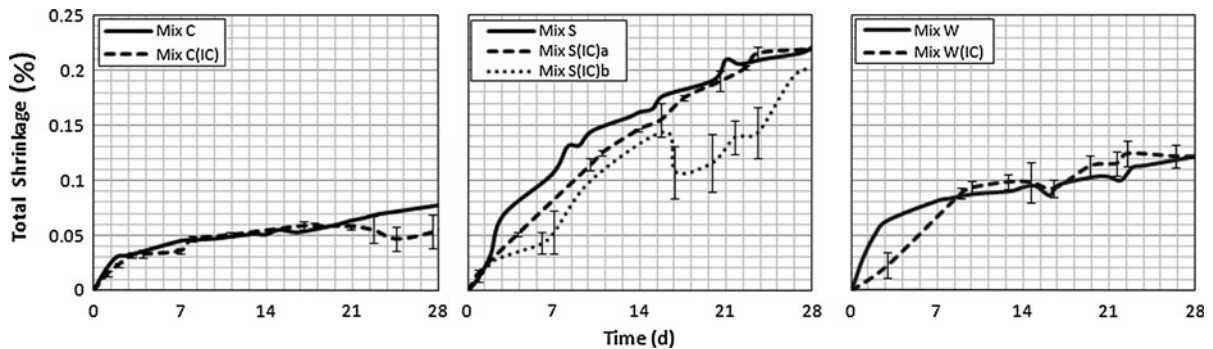


Fig. 7 Total shrinkage of the control, Na_2CO_3 activated, and waterglass/NaOH activated mixes (mixes C, S, and W, respectively) with and without internal curing. All scales are

equal. *Error bars* represent measured standard deviation; *curves without error bars* are an average of two specimens

total shrinkage of mixture C(IC) dipped slightly, along with an increase in experimental error. As the shrinkage of mixtures C and C(IC) continued to increase at the same rate after roughly 25 days, this dip is more likely due to experimental error than to any substantial action on the part of the internal curing. Similar curves are observed for the mixtures activated by the waterglass/NaOH solution, which reach shrinkages of 0.12 % after 28 days. Internal curing may have delayed the onset of shrinkage slightly, but the data have converged after an age of 8 days.

The mixtures activated by Na_2CO_3 solution had the highest levels of total shrinkage, passing 2 % after 28 days (Fig. 7). The two mixtures containing internal curing, S(IC)a (with water as the internal curing agent) and S(IC)b (with Na_2CO_3 solution as the internal curing agent) showed slight reductions in shrinkage, but not enough to be statistically meaningful. (The origin of the substantial, sudden decrease in the total shrinkage of mixture S(IC)b starting at 17 days is not clear, but is conjectured to be an artifact introduced during the experiments.)

That internal curing had negligible effect on the total shrinkage of the three mixtures, while effectively eliminating autogenous shrinkage, implies that drying shrinkage is the dominant factor in all three mixtures when exposed to a 50 % RH environment.

For the control mixture, a variety of drying shrinkage mitigation methods are available, including the use of water-reducing admixtures, shrinkage-reducing admixtures, and using a lower water:cement ratio. (The water:cement ratio used here, 0.45, is somewhat on the high end, and was chosen to match that of mixture S.) These methods would reduce the amount of evaporable water available to the system, leading to less water exiting the body during drying, and lowered rates of shrinkage.

Shrinkage mitigation methods for the two alkali-activated slags are more complicated; it is known that various admixtures commonly used in cements may not work effectively in alkali-activated systems [18, 27, 38]. Reducing the activator:slag ratio does not immediately appear to be a viable option, as lower ratios investigated early in this project were not

workable. However, it is known that metakaolin-based geopolymers undergo substantial changes in rheology; as the activator dissolves metakaolin particles over time, the mixture becomes more and more workable [37]. For this reason, mixtures that initially appear workable become ‘soupy’ over time, leading to poor early-age properties, while a properly-proportioned mix will initially appear quite dry and only be ready for placement after the activator has had some amount of time to react with the metakaolin. This is one reason (of several) that interest has largely shifted from metakaolin to fly ash as a geopolymer precursor. Such an effect *may* be present in the alkali-activated slags, which would mean that the activator:slag ratio could be reduced. Further rheological studies are necessary to examine this issue, and even if possible, such a reduction may not be practical, as in the case of metakaolin-based geopolymers.

4 Conclusions

Alkali activated slags are an alternative binder system that shows considerable promise as environmentally friendly building materials. However, shrinkage of these systems is poorly understood and remains an obstacle to widespread adoption. Internal curing has been shown to be a simple, effective method by which autogenous shrinkage can be effectively mitigated, even in systems using an activating solution with a high pH and high levels of reactive silica, in which autogenous shrinkage is substantially more pronounced than in control mixtures. In the mixtures examined here, drying shrinkage was the main shrinkage mechanism, due to the amount of activating solution used. Though autogenous shrinkage can be easily addressed with internal curing, the mitigation of drying shrinkage will require (a) the development of shrinkage-reducing admixtures that perform as well in alkali-activated slags as they do in OPC-based systems, and/or (b) a more complete understanding of the evolution of rheological properties in alkali activated slags (and thus development of mixtures with a lower activator:slag ratio).

5 Acknowledgments

This research was supported by a grant from the National Research Council’s Research Associateship

Program. The authors would like to thank Big River Industries, Holcim US Inc., and PQ Corporation for providing samples.

References

1. Akcay B, Tasdemir MA (2010) Effects of distribution of lightweight aggregates on internal curing of concrete. *Cement Concr Compos* 32(8):611–616. doi:[10.1016/j.cemconcomp.2010.07.003](https://doi.org/10.1016/j.cemconcomp.2010.07.003)
2. Altan E, Erdoğan ST (2012) Alkali activation of a slag at ambient and elevated temperatures. *Cem Concr Compos* 34(2):131–139. doi:[10.1016/j.cemconcomp.2011.08.003](https://doi.org/10.1016/j.cemconcomp.2011.08.003)
3. ASTM International (1995) Standard test method for density of hydraulic cement. C188-95. ASTM International, West Conshohocken
4. ASTM International (2007) Standard test method for chemical shrinkage of hydraulic cement paste. ASTM C1608-07. ASTM International, West Conshohocken
5. ASTM International (2009) Specification for lightweight aggregate for structural concrete. ASTM C330/C330M-09. ASTM International, West Conshohocken
6. ASTM International (2009) Standard test method for autogenous strain of cement paste and mortar. ASTM C1698-09. ASTM International, West Conshohocken
7. ASTM International (2009) Standard test method for drying shrinkage of mortar containing hydraulic cement. ASTM C596-09. ASTM International, West Conshohocken
8. ASTM International (2011) Standard test method for compressive strength of hydraulic cement mortars (using 2-in. or [50-mm] cube specimens). ASTM C109/C109M-11a. ASTM International, West Conshohocken
9. Bakharev T, Sanjayan JG, Cheng YB (2001) Resistance of alkali-activated slag concrete to alkali-aggregate reaction. *Cem Concr Res* 31(2):331–334. doi:[10.1016/s0008-8846\(00\)00483-x](https://doi.org/10.1016/s0008-8846(00)00483-x)
10. Bakharev T, Sanjayan JG, Cheng YB (2003) Resistance of alkali-activated slag concrete to acid attack. *Cem Concr Res* 33(10):1607–1611. doi:[10.1016/s0008-8846\(03\)00125-x](https://doi.org/10.1016/s0008-8846(03)00125-x)
11. Bentz DP, Snyder KA (1999) Protected paste volume in concrete: extension to internal curing using saturated lightweight fine aggregate. *Cem Concr Res* 29(11):1863–1867. doi:[10.1016/s0008-8846\(99\)00178-7](https://doi.org/10.1016/s0008-8846(99)00178-7)
12. Bentz DP, Weiss WJ (2011) Internal curing: a 2010 state-of-the-art-review, NISTIR 7765. U.S. Department of Commerce
13. Bentz DP, Lura P, Roberts JW (2005) Mixture proportioning for internal curing. *Concr Int* 27(2):35–40
14. Bentz DP, Halleck PM, Grader AS, Roberts JW (2006) Water movement during internal curing: direct observation using X-ray microtomography. *Concr Int* 28(10):39–45
15. Brough AR, Atkinson A (2002) Sodium silicate-based, alkali-activated slag mortars: part I. Strength, hydration and microstructure. *Cem Concr Res* 32(6):865–879
16. Bullard JW, Enjolras E, George WL, Satterfield SG, Terrill JE (2010) A parallel reaction-transport model applied to cement hydration and microstructure development. *Modell Simul Mater Sci Eng* 18(2):025007



17. Castro J, Keiser L, Golias M, Weiss J (2011) Absorption and desorption properties of fine lightweight aggregate for application to internally cured concrete mixtures. *Cement Concr Compos* 33(10):1001–1008. doi:[10.1016/j.cemconcomp.2011.07.006](https://doi.org/10.1016/j.cemconcomp.2011.07.006)
18. Criado M, Palomo A, Fernández-Jiménez A, Banfill P (2009) Alkali activated fly ash: effect of admixtures on paste rheology. *Rheol Acta* 48(4):447–455. doi:[10.1007/s00397-008-0345-5](https://doi.org/10.1007/s00397-008-0345-5)
19. Dunster AM (2008) Recycled gypsum in concrete construction product applications. Waste & Resources Action Programme, Banbury
20. Duxson P, Provis JL (2008) Low CO₂ concrete: are we making any progress? In: BEDP environment design guide. Royal Australian Institute of Architects, Darwin
21. Duxson P, Fernández-Jiménez A, Provis JL, Lukey GC, Palomo A, Deventer JSJ (2007) Geopolymer technology: the current state of the art. *J Mater Sci* 42(9):2917–2933
22. Duxson P, Fernández-Jiménez A, Provis JL, Lukey GC, Palomo A, van Deventer JSJ (2007) Geopolymer technology: the current state of the art. *J Mater Sci* 42:2917–2933
23. Duxson P, Provis JL, Lukey GC, van Deventer JSJ (2007) The role of inorganic polymer technology in the development of ‘green concrete’. *Cem Concr Res* 37(12):1590–1597. doi:[10.1016/j.cemconres.2007.08.018](https://doi.org/10.1016/j.cemconres.2007.08.018)
24. Feng X, Garboczi EJ, Bentz DP, Stutzman PE, Mason TO (2004) Estimation of the degree of hydration of blended cement pastes by a scanning electron microscope point-counting procedure. *Cem Concr Res* 34(10):1787–1793. doi:[10.1016/j.cemconres.2004.01.014](https://doi.org/10.1016/j.cemconres.2004.01.014)
25. Gartner E (2004) Industrially interesting approaches to “low-CO₂” cements. *Cem Concr Res* 34(9):1489–1498. doi:[10.1016/j.cemconres.2004.01.021](https://doi.org/10.1016/j.cemconres.2004.01.021)
26. Golias M, Bentz DP, Weiss J (2012) Influence of exposure conditions on the efficacy of internal curing. *Adv Civ Eng Mater* (submitted)
27. Habert G, d’Espinose de Lacaillerie JB, Roussel N (2011) An environmental evaluation of geopolymer based concrete production: reviewing current research trends. *J Clean Prod* 19(11):1229–1238. doi:[10.1016/j.jclepro.2011.03.012](https://doi.org/10.1016/j.jclepro.2011.03.012)
28. Hendriks CA, Worrell E, Jager Dd, Blok K, Riemer P (2004) Emission reduction of greenhouse gases from the cement industry. Paper presented at the Proceedings of the 7th international conference on greenhouse gas control technologies, Vancouver, Canada, Sept. 5–9, 2004
29. Hubler MH, Thomas JJ, Jennings HM (2011) Influence of nucleation seeding on the hydration kinetics and compressive strength of alkali activated slag paste. *Cem Concr Res* 41(8):842–846. doi:[10.1016/j.cemconres.2011.04.002](https://doi.org/10.1016/j.cemconres.2011.04.002)
30. Jensen OM, Hansen PF (2001) Water-entrained cement-based materials: I. Principles and theoretical background. *Cem Concr Res* 31(4):647–654. doi:[10.1016/s0008-8846\(01\)00463-x](https://doi.org/10.1016/s0008-8846(01)00463-x)
31. Jensen OM, Hansen PF (2002) Water-entrained cement-based materials: II. Experimental observations. *Cem Concr Res* 32(6):973–978. doi:[10.1016/s0008-8846\(02\)00737-8](https://doi.org/10.1016/s0008-8846(02)00737-8)
32. Juenger MCG, Winnefeld F, Provis JL, Ideker JH (2011) Advances in alternative cementitious binders. *Cem Concr Res* 41(12):1232–1243. doi:[10.1016/j.cemconres.2010.11.012](https://doi.org/10.1016/j.cemconres.2010.11.012)
33. Lecomte I, Henrist C, Liegéois M, Maseri F, Rulmont A, Cloots R (2006) (Micro)-structural comparison between geopolymers, alkali-activated slag cement and portland cement. *J Eur Ceram Soc* 26:8
34. Melo Neto AA, Cincotto MA, Repette W (2008) Drying and autogenous shrinkage of pastes and mortars with activated slag cement. *Cem Concr Res* 38(4):565–574. doi:[10.1016/j.cemconres.2007.11.002](https://doi.org/10.1016/j.cemconres.2007.11.002)
35. Palacios M, Puertas F (2007) Effect of shrinkage-reducing admixtures on the properties of alkali-activated slag mortars and pastes. *Cem Concr Res* 37(5):691–702. doi:[10.1016/j.cemconres.2006.11.021](https://doi.org/10.1016/j.cemconres.2006.11.021)
36. Phair JW (2006) Green chemistry for sustainable cement production and use. *Green Chem* 8(9):763–780
37. Provis JL, Duxson P, van Deventer JSJ (2010) The role of particle technology in developing sustainable construction materials. *Adv Powder Technol* 21(1):2–7. doi:[10.1016/j.apt.2009.10.006](https://doi.org/10.1016/j.apt.2009.10.006)
38. Rees CA, Provis JL, Lukey GC, van Deventer JSJ (2008) The mechanism of geopolymer gel formation investigated through seeded nucleation. *Colloids Surf A* 318(1–3):97–105. doi:[10.1016/j.colsurfa.2007.12.019](https://doi.org/10.1016/j.colsurfa.2007.12.019)
39. Sakulich AR (2011) Reinforced geopolymer composites for enhanced material greenness and durability. *Sustain Cities Soc* 1(4):195–210. doi:[10.1016/j.scs.2011.07.009](https://doi.org/10.1016/j.scs.2011.07.009)
40. Sakulich AR, Anderson E, Schauer C, Barsoum MW (2009) Mechanical and microstructural characterization of an alkali-activated slag/limestone fine aggregate concrete. *Constr Build Mater* 23(8):2951–2957. doi:[10.1016/j.conbuildmat.2009.02.022](https://doi.org/10.1016/j.conbuildmat.2009.02.022)
41. Sakulich AR, Miller S, Barsoum MW (2010) Chemical and microstructural characterization of 20-month-old alkali-activated slag cements. *J Am Ceram Soc* 93(6):1741–1748. doi:[10.1111/j.1551-2916.2010.03611.x](https://doi.org/10.1111/j.1551-2916.2010.03611.x)
42. Sanjuán MA, Zaragoza A, López Agüí JC (2011) Standardization for an innovative world. *Cem Concr Res* 41(7):767–774. doi:[10.1016/j.cemconres.2011.03.015](https://doi.org/10.1016/j.cemconres.2011.03.015)
43. Shi C, Day RL (1995) A calorimetric study of early hydration of alkali-slag cements. *Cem Concr Res* 25(6):13
44. Shi C, Krivenko PV, Roy DM (2006) Alkali-activated cements and concretes. Taylor and Francis, New York
45. Thomas JJ, Allen AJ, Jennings HM (2012) Density and water content of nanoscale solid C–S–H formed in alkali-activated slag (AAS) paste and implications for chemical shrinkage. *Cem Concr Res* 42(2):377–383. doi:[10.1016/j.cemconres.2011.11.003](https://doi.org/10.1016/j.cemconres.2011.11.003)
46. Trtik P, Münch B, Weiss WJ, Kaestner A, Jerjen I, Josic L, Lehmann E, Lura P (2011) Release of internal curing water from lightweight aggregates in cement paste investigated by neutron and X-ray tomography. *Nucl Instrum Methods Phys Res A* 651(1):244–249. doi:[10.1016/j.nima.2011.02.012](https://doi.org/10.1016/j.nima.2011.02.012)
47. van Oss HG (2011) Cement. USGS mineral commodity survey. United States Geological Survey, Reston
48. Winnefeld F, Lothenbach B (2010) Hydration of calcium sulfoaluminate cements—experimental findings and thermodynamic modelling. *Cem Concr Res* 40(8):1239–1247. doi:[10.1016/j.cemconres.2009.08.014](https://doi.org/10.1016/j.cemconres.2009.08.014)
49. Woltron G (2009) The utilisation of GGBFS for advanced supersulfated cements. *World Cement Magazine SEP*:157–162

-
50. Worrell E, Price L, Martin N, Hendriks C, Meida LO (2001) Carbon dioxide emissions from the cement industry. *Annu Rev Energy Env* 26(1):303–329. doi:[10.1146/annurev.energy.26.1.303](https://doi.org/10.1146/annurev.energy.26.1.303)
51. Xu H, Provis JL, Deventer JSJv, Krivenko PV (2008) Characterization of aged slag concretes. *ACI Mater J* 105(2):131–139